scientific reports

Check for updates

OPEN

Enamel carbon, oxygen, and strontium isotopes reveal limited mobility in an extinct rhinoceros at Ashfall Fossil Beds, Nebraska, USA

Clark T. Ward[1,5]✉, Brooke E. Crowley[1,2] & Ross Secord[3,4]

Ashfall Fossil Beds in Nebraska, USA, was a mid-Miocene (11.86 ± 0.13 Ma) watering-hole that preserved hundreds of herbivores in volcanic ash. The short-legged, barrel-bodied rhinoceros, *Teleoceras major* (Mammalia; Rhinocerotidae), is abundant at Ashfall (> 100 individuals), leading some researchers to suggest individuals formed large groups, while others have argued they congregated at Ashfall seeking refuge from the ash that ultimately caused their death. Here, we evaluated three types of mobility—natal dispersal of subadults, seasonal migration, and response to natural disaster—using carbon, oxygen, and strontium isotope ratios in tooth enamel from thirteen *T. major* adult individuals. We bulk and serially sampled enamel from mandibular second and third molars, which should respectively record behaviour after weaning but before and after possible natal dispersal. Results indicate that all sampled individuals had limited mobility and were local to Ashfall. Semi-aquatic adaptations likely restricted *T. major* to wet habitats and prohibited long-distance movement. Social (rather than spatial) dispersal, seasonal dietary flexibility, and elevated Miocene primary productivity could have allowed individuals to maintain genetic diversity and avoid depleting local resources. Reconstructing how extinct ungulates utilized ancient landscapes provides important context for understanding their paleoecology and sociality as well as the environments they inhabited.

Keywords Dispersal, Landscape use, Miocene, Seasonal migration, Serial sampling, Ungulate

Large terrestrial herbivores (particularly hooved ungulates) have considerable impacts on the ecosystems they inhabit. Ungulate herbivory and nutrient cycling greatly influence vegetation structure and, in turn, modulate plant and small animal diversity as well as fire regimes[1–3]. Savanna ecosystems—grassy biomes with scattered open canopy forests—are particularly strongly affected by herbivory[1–3]. Consequently, tracking herbivore mobility and landscape use can provide key insights into savanna ecosystem processes[1–3]. It is unknown if landscape use and mobility patterns observed in modern savannas apply to ancient environments, such as the highly diverse savanna-woodlands of mid-Miocene (ca. 16–11.5 Ma) central North America[4–6]. Miocene and modern ungulate communities have similar ecomorphological composition[4–6], but a warm and equable climate may have influenced Miocene vegetation productivity and availability, which in turn could have impacted ungulate behaviour.

Here, we use carbon ($\delta^{13}C$), oxygen ($\delta^{18}O$), and strontium isotope ratios ($^{87}Sr/^{86}Sr$) in bulk and serially sampled molar enamel to evaluate mobility in the extinct rhinoceros, *Teleoceras major*, from the mid-Miocene Ashfall Fossil Beds, Nebraska, USA (henceforth referred as "Ashfall"; Fig. 1). We consider three types of mobility: (1) dispersal from a natal area as a subadult to avoid intraspecific competition and minimize inbreeding upon sexual maturity; (2) seasonal migration following availability of water and preferred foods; and (3) long-distance movement in response to a major environmental perturbation or catastrophe.

Overview of ungulate mobility

The degree of mobility undertaken by an herbivore species depends on its social structure, diet, and body size. Generally, "dispersal" refers to long-distance movements of subadults from their natal area to their first breeding

[1]Department of Geosciences, University of Cincinnati, Cincinnati, OH 45221, USA. [2]Department of Anthropology, University of Cincinnati, Cincinnati, OH 45221, USA. [3]Department of Earth and Atmospheric Sciences, University of Nebraska–Lincoln, Lincoln, NE 68588, USA. [4]Division of Vertebrate Paleontology, University of Nebraska State Museum, Lincoln, NE 68588, USA. [5]Present address: Department of Earth and Environmental Sciences, University of Minnesota, Minneapolis, MN 55455, USA. ✉email: ward1179@umn.edu

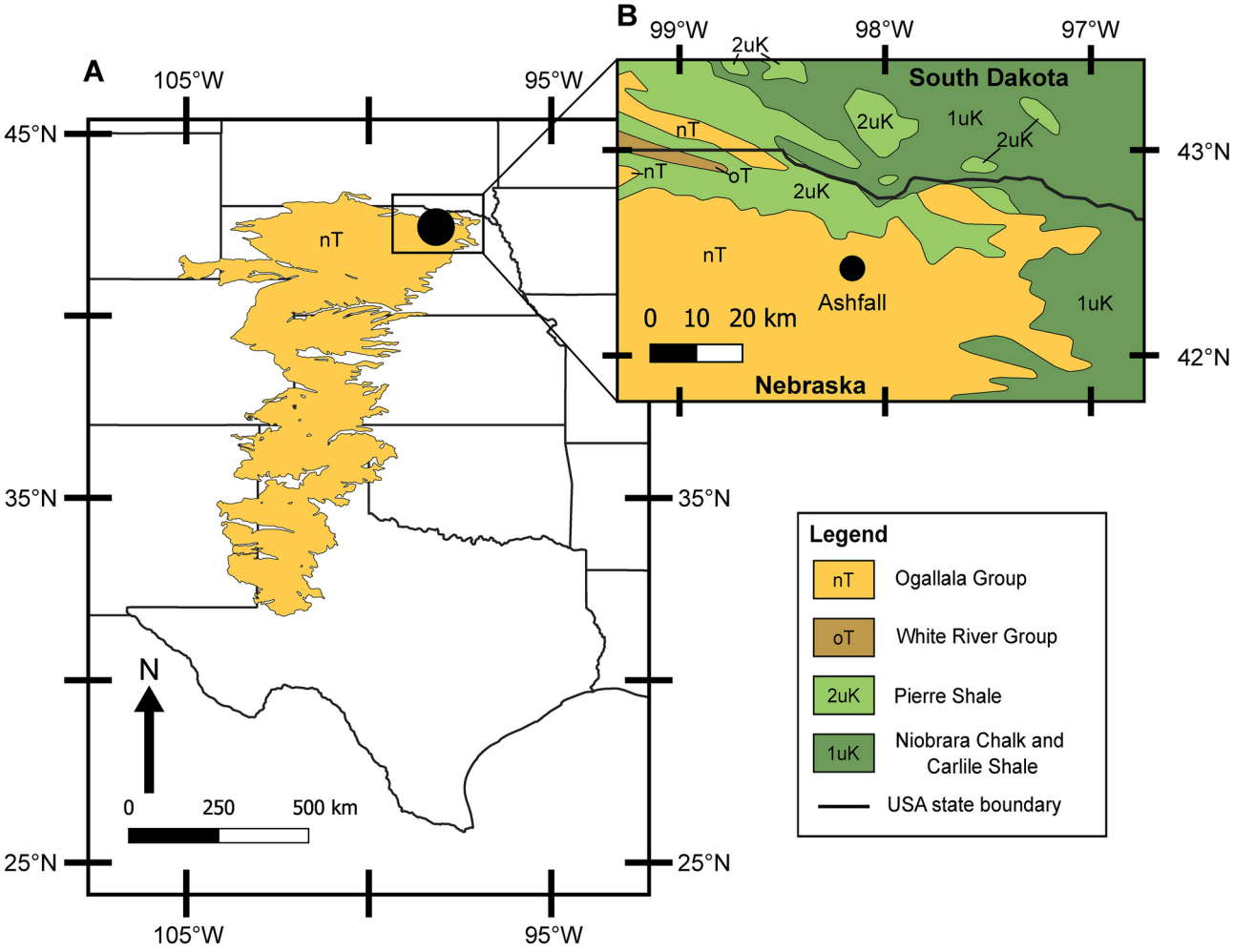

Fig. 1. Maps of (**A**) the central midwestern USA showing state boundaries, the extent of the Neogene Ogallala Group, and location of Ashfall Fossil Beds State Historical Park ("Ashfall"; filled circle); and (**B**) regional bedrock geology in north-central Nebraska and south-central South Dakota. Figure made with QGIS 3.22.9 (https://www.qgis.org); bedrock map GIS files sourced from the United States Geological Survey National Geologic Map Database (public domain). Modified from Ward et al.[29].

area (called natal dispersal), but adults may also disperse between breeding cycles to avoid competition and inbreeding (breeding dispersal)[7]. Among monogamous ungulate species, offspring of both sexes disperse to reduce competition for resources and mates[7,8]. However, in many modern large ungulate species, only a small proportion of males successfully mate with the majority of females (polygyny). This leads to competition between males for mating rights, which in turn leads to selection for sexual dimorphism by exaggerated traits used in display or combat[7–9]. Polygyny also leads to sex-biased dispersal; males are more frequently the dispersing sex, while female offspring often remain near their natal range (philopatry)[7–9]. In contrast, in polygynous species where males defend territories or resources (resource defence polygyny), it is common for both male and female subadults to disperse and establish home ranges elsewhere[9]. Female-biased dispersal may evolve, but it is relatively rare among mammals and has only been observed once in extant ungulates (feral horses; *Equus caballus*)[9].

Seasonal migration is driven by the seasonal availability of a species' preferred food and water, which in turn are driven by fluctuations in temperature and precipitation. At higher latitudes, seasonality is pronounced, and thus ungulates are more likely to move seasonally than those at lower latitudes[10,11]. Ungulates cope with a seasonal dearth of food and water by spatially following the growth of preferred forage (resource tracking) or by staying in place and changing preferred forage type (diet switching)[10,11]. Resource tracking, and therefore migration, is most often observed in grass-dependent herbivores (grazers), which follow seasonal "waves" of fresh grass growth[10–12]. In contrast, browsers (leafy vegetation consumers) are typically non-migratory and are able to maintain their preferred diet[10,11]. This is because deeply rooted woody shrubs and trees are more likely to access permanent water sources (i.e., groundwater) than grasses[13,14]. Mixed-feeding herbivores tend to switch their diets seasonally, foraging on grasses during the growing season and more leafy dicot vegetation during other seasons[10,11]. Finally, larger ungulates have larger body fat reserves, are capable of eating less nutritious foods, and are physically more capable of traversing longer distances than smaller species[15]. Thus,

megaherbivores (≥1000 kg) are more likely to migrate longer distances than smaller ones[10,11,15]. During the mid-Miocene, North America was at similar mid-latitudes to today, but the climate was relatively warm and equable. The mid-Miocene supported a greater diversity of ungulates than any modern savanna, potentially because of elevated primary productivity and reduced seasonality[16,17]. Reduced seasonal shifts in vegetation availability may have allowed ancient herbivores to stay in place year-round[4,16]. In support of this possibility, recent ancestral state reconstructions of extant ungulates suggest that seasonal migration may have originated during the mid-Miocene[11].

Environmental perturbations like droughts, floods, or other natural disasters can greatly affect herbivore landscape use patterns. How ungulates respond to environmental perturbations is expected to vary depending on the type of disaster, diet, and body size[18,19]. During droughts, grazers tend to move long distances in search of less affected habitats, while browsers that consume deep-rooted woody vegetation maintain their preferred diet and are less likely to move[18]. In contrast, during catastrophic floods, terrestrial herbivores must move away from inundated low-lying areas[19]. Depending on the vegetation present on higher and drier grounds, animals may be forced to shift their diet to include more or less woody vegetation or risk starvation[19]. In this study, we investigated the local effects of a supervolcano eruption that blanketed most of western North America with ca. 650 km^3 of ejecta[20–22]. It is unknown if the ash impacted all animals regardless of their adaptations or if certain traits influenced survivorship. For example, as noted above, megaherbivores may have been able to travel longer distances in search of refugia than smaller species[15,18,19].

Isotope background

Carbon isotope ratios in herbivore enamel reflect consumed vegetation. Typically, researchers use $\delta^{13}C$ values to distinguish consumption of C_3 and C_4 foods[23,24]. During the mid-Miocene, C_4 plants comprised ≤20% of total plant biomass and contributed negligibly to herbivore diet[16,25–27]. Nevertheless, carbon isotope values can still help distinguish herbivores that foraged on C_3 plants in different environments[28]. Ward et al.[29] previously found that all ungulates at Ashfall, including adult *Teleoceras major*, foraged on C_3 plants in relatively open habitats, but it is possible that some individuals foraged in different habitats earlier in life. Carbon isotope values may also be able to track seasonal variability in consumed foods, but the magnitude of this variability is expected to be small (ca. 1–2‰)[28], particularly during the mid-Miocene when seasonality was more moderate[16,17,30]. We therefore expect $\delta^{13}C$ to be of less utility than $\delta^{18}O$ or $^{87}Sr/^{86}Sr$ for identifying behavioural shifts or tracking landscape use in *T. major* at Ashfall, but we include it nevertheless to provide corroborative support for patterns observed in other isotopes.

Oxygen isotope values in large herbivores like rhinoceroses are primarily influenced by drinking water, and to a lesser extent thermoregulatory mechanisms and water in consumed vegetation[31,32]. Evaporation (and evapotranspiration) preferentially remove $H_2{}^{16}O$, such that $\delta^{18}O$ values of drinking water and leaf water increase with higher temperature or lower relative humidity[33–36]. Oxygen isotopes can thus illuminate niche partitioning among co-occurring animals (e.g., those that prefer wet versus dry habitats) as well as seasonal variations in temperature and precipitation (warm/dry vs. cool/wet seasons)[37–40]. Additionally, semi-aquatic animals that spend a lot of time in the water, like the modern common hippopotamus (*Hippopotamus amphibius*), have $\delta^{18}O$ values that reflect $\delta^{18}O$ trends in meteoric water and may be lower than co-occurring terrestrial ungulates[37,40,41].

Strontium isotope ratios in tooth enamel can track the geographic location(s) where an animal foraged during the time of tooth mineralization[42]. This is because $^{87}Sr/^{86}Sr$ in tooth enamel reflects consumed vegetation and drinking water[42], and the primary source of Sr to plants and water is weathered sediments and bedrock. Biologically available $^{87}Sr/^{86}Sr$ varies with both age and mineral composition of the parent rock[43]. Additional sources of Sr to biological systems include atmospheric Sr (e.g., dust, aerosols, sea spray, etc.) and transported aqueous Sr in groundwater or rivers and streams[44–47]. Strontium isotopes on their own can reveal spatial niche partitioning, as well as shifts in landscape use during life, and they are even more effective when paired with $\delta^{18}O$ data[29,48–53].

Predictions of mobility for *Teleoceras major*

Teleoceras major was a species of barrel-bodied, short-legged rhinoceros endemic to North America during the Clarendonian North American land mammal age (12.5–10 Ma)[54,55]. All *Teleoceras* species had sexually dimorphic lower second incisors (I_2's or "tusks"); females possessed smaller rounded tusks while males had larger pointed tusks[56,57] (Fig. 2). This type of sexual dimorphism strongly suggests polygyny; males likely used their sharp, enlarged tusks in agonistic displays and combat to secure mating privileges[56,58,59]. Thus, we predict male-biased natal dispersal in *T. major*, but evaluating this for an extinct species is challenging[9]. At Ashfall, the majority of uncovered skeletons were reproductive females, their calves, and immature females[21,59]. There are several older, likely dominant males, but subadult males are absent[21,59]. Voorhies[59] suggested that subadult males were driven away by the dominant males and lived elsewhere. Similarly, Mihlbachler[58] interpreted male-biased mortality of subadult and young adult *T. proterum* at Love Bone Bed and Mixon's Bone Bed in Florida (ca. 9 and 8 Ma, respectively) to indicate that subadult males suffered increased mortality after dispersal (common among modern mammals[8]). Young adult males participated in deadly combat and may have lived under suboptimal conditions to avoid dominant adults[58]. Additionally, enamel hypoplastic deformities (evidence of severe physiological stress) were observed on isolated Nebraskan *Teleoceras* permanent fourth premolars (P_4's)[60]. It is plausible these hypoplasias reflect stress endured during dispersal, but it is unknown if this dental pathology was limited to males or occurred in both sexes[58,60–62].

Inferred *Teleoceras* sociality differed from modern rhinoceros species, which are typically solitary but occasionally form small, ephemeral groupings[63]. Most modern species are polygynous, but mating behaviour has not been studied in wild Sumatran rhinoceroses (*Dicerorhinus sumatrensis*) nor Javan rhinoceroses (*Rhinoceros sondaicus*). Some species have similar tusk and body size dimorphism to *Teleoceras* (e.g., greater one-horned

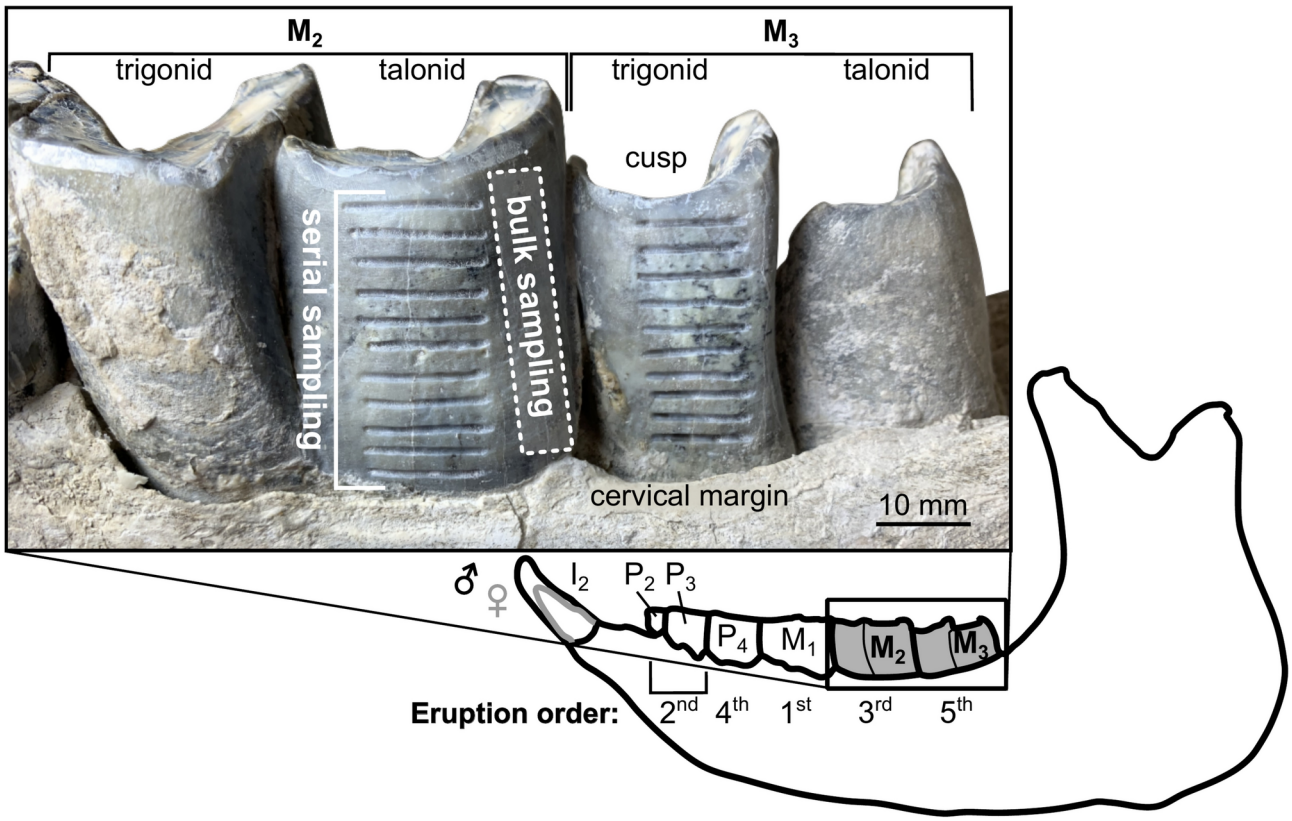

Fig. 2. Diagram showing *Teleoceras* tooth eruption sequence and methodology used for bulk and serial sampling of tooth enamel. I_2 = second incisor; P_2 = second premolar; P_3 = third premolar; P_4 = fourth premolar; M_1 = first molar; M_2 = second molar; M_3 = third molar. Shaded molars (M_2 and M_3) were sampled. I_2 outlines illustrate sexual dimorphism. Eruption order of permanent teeth from refs[58,60–62]. Bulk sampling incorporated enamel from the entire height of the tooth, while serial sampling targeted discrete bands of enamel perpendicular to the growth axis; see Methods for details. Bulk sampling was done on readily accessible surfaces, but only M_3 trigonids and M_2 talonids were serially sampled. Photographs by CTW, used with permission from the University of Nebraska State Museum.

rhinoceros, *Rhinoceros unicornis*), while others have monomorphic body sizes and lack tusks entirely (e.g., black rhinoceros, *Diceros bicornis*)[64,65]. In modern species, weaned juveniles of both sexes are separated from their mothers (cow-calf separation) days before the next calf is born, at ca. two years old. These subadults then typically disperse prior to reaching maturity (ca. seven to ten years old depending on species and sex)[63,64,66].

The *Teleoceras* genus is recognized by its shortened leg and foot bones (brachypody) and tall-crowned molars (hypsodonty)[54]. Hypsodont molars are an adaptation for a grass-heavy diet, and Voorhies and Thomasson[67] found silicified grass macrofossils (*Berriochloa* spp.) in the oral and gut cavities of *T. major* skeletons at Ashfall, which confirmed that some individuals ate grass. However, dental micro- and mesowear analyses indicate that *T. major* at Ashfall was likely a mixed-feeder, consuming some leafy vegetation in addition to grass[68]. There is thus mixed dietary evidence supporting seasonal migration. Additionally, possible reduced seasonality during the mid-Miocene could have lessened the need for *T. major* to move seasonally, even if it primarily consumed grass. Large body mass may also suggest seasonal migration[10,11], although estimated masses (880–1110 kg for males and 785–840 kg for females[56]) are near or just below the cut-off typically used to define a megaherbivore[15]. Lastly, brachypody is the opposite of what is expected for a highly mobile animal (i.e., gracility)[69]. The evolutionary function of brachypody in *Teleoceras* is not well understood, but has been suggested to be an adaptation for grazing or semi-aquatic behaviour (similar to the modern common hippopotamus)[69]. Recent isotopic evidence supports a semi-aquatic lifestyle for *T. major* at Ashfall[29].

Lastly, it is possible that the *Teleoceras major* preserved at Ashfall travelled long distances in response to a large, catastrophic volcanic eruption derived from the Yellowstone-hotspot dated to 11.86 ± 0.13 Ma[20,22]. Voorhies[59] interpreted the large number of preserved *T. major* individuals as a permanent, large herd that was "frozen in time". In contrast, Mihlbachler[58] suggested that *T. major* was typically solitary (like modern rhinoceroses) but congregated at Ashfall from the larger surrounding region between initial ash fall and death. At Ashfall, vertebrate skeletons are entombed in a lens of glassy, volcanic ash that filled a low-lying depression, which is interpreted as an ephemeral watering-hole[21,59]. The ash rapidly killed and buried the smallest organisms (turtles, birds, and small ruminant artiodactyls). Medium-sized ungulates (horses and camels) died next and were buried in subsequent wind-blown ash. *Teleoceras major* was the last ungulate species to perish and to be buried by wind-

blown ash. This eruption would have blanketed all vegetation and buried low-growing forage (grasses, forbs, sedges, etc.) in 20–30 cm of fine ash, eliminating most or all available forage[21,59]. Furthermore, pathologic bone growths (the result of inhaling copious amounts of ash) indicate that *T. major* individuals preserved at Ashfall may have survived for a few weeks following initial ash fall[21,59]. Therefore, there was a short period of time where *T. major* could have immigrated from elsewhere in search of refuge from the ash and relief from symptoms caused by ash inhalation and subsequent bone growths (including fever, arthritis, swelling of the limbs, and lethargy)[21,59].

To investigate mobility in *Teleoceras major*, we first tested for dispersal by comparing bulk sampled permanent mandibular second and third molars (M_2's and M_3's, respectively; Fig. 2) of five males and eight females (M_3 data previously published in Ward et al.[29]). Both teeth should have formed after weaning[58,60–62] and represent adult diets[70]. M_2's and M_3's mineralized before and after P_4 formation, respectively[58,60–62], and thus, if dispersal occurred during or soon after cow-calf separation in *T. major*, we should find ecologically meaningful isotopic differences between M_2's and M_3's, particularly in males. Bulk sampling of multiple individuals reveals broad patterns in niche partitioning and landscape use (Fig. 2). In contrast, serial sampling enamel in discrete bands from cusp to the cervical margin along a tooth crown tracks isotopic patterns as the tooth mineralizes[38,71] (Fig. 2). Due to the two-phased mineralization of enamel, serial sampling provides attenuated signals of short-term changes, but should retain evidence of longer-term (e.g., seasonal) shifts[38,71–74]. We tested for seasonal migration by serially sampling M_2's and M_3's from two male and two female *Teleoceras major*. We visually evaluated patterns within and between teeth for each individual, as well as between individuals and sexes. Lastly, we tested for long-distance movement in response to inundation of volcanic ash by comparing (1) isotope data for bulk and serially sampled molars from *T. major* with previously published data for co-occurring ungulates (from Ward et al.[29]), and (2) the range in $^{87}Sr/^{86}Sr$ for *T. major* as well as all Ashfall ungulates with the expected range in bioavailable $^{87}Sr/^{86}Sr$ in the Ashfall region based on a modern $^{87}Sr/^{86}Sr$ isoscape from Reich et al.[75].

Materials and methods

Site description

Ashfall Fossil Beds State Historical Park is located in Antelope County, Nebraska, USA (42.420° N, 98.156° W; Fig. 1). Fossils from a variety of mammals, birds, and reptiles are preserved in the lowest meter of a three-meter-thick lens of volcanic ash, derived from the Bruneau-Jarbidge Volcanic Field in the Snake River Province in southwestern Idaho; zircons from the ash were U–Pb dated to 11.86 ± 0.13 Ma[20,21,59]. This ash lens is found within the Cap Rock Member of the Ash Hollow Formation of the Ogallala Group (Fig. 1). The Cap Rock Member is comprised of silty sandstones that were interpreted as floodplain deposits, and the low lying area filled with ash is interpreted as a watering-hole[21,59]. The preserved mammalian fauna is dominated by medium to large ungulates, including *Teleoceras major* (Rhinocerotidae), five horse genera (Equidae; *Cormohipparion*, *Neohipparion*, *Pseudhipparion*, *Pliohippus*, and *Protohippus*), two camel genera (Camelidae; *Procamelus* and *Protolabis*), and one genus of ruminant artiodactyl (Blastomerycinae; *Longirostromeryx*). It is placed in the medial biochron of the Clarendonian North American land mammal age (12–10 Ma)[21,55]. A paleoecological review of these genera (except *Neohipparion* and *Protohippus*) can be found in Ward et al.[29] We also refer the reader to other literature that reviews Ashfall in more detail[21,29,59].

Materials

Sampled specimens are housed in the Division of Vertebrate Paleontology at the University of Nebraska State Museum (UNSM). We selected 13 complete mandibles from eight female and five male *Teleoceras major* adults; this was the maximum number of adult male mandibles available ex situ in the UNSM collections. We worked with complete mandibles because they retain the sexually dimorphic lower second incisors (I_2's; Fig. 2), which allowed for sex determination[56]. We sampled bulk enamel from both M_2's and M_3's from all selected specimens. We also serially sampled M_2's and M_3's from two males, Woofy (UNSM 52247) and Grandpa John (UNSM 27805), and two females, Mary Anning (UNSM 52286) and Sparky (UNSM 27807). We chose these individuals because they had fully erupted, yet minimally worn, molars.

Powdered enamel was removed from the teeth using a variable-speed dental drill with a 1 mm diamond burr. Before collecting powder for analysis, we removed ca. 0.5 mm of the outer surface of each tooth to reveal pristine enamel in the area sampled. Enamel was tested for hardness by scratching with a carbide pick mounted in a pin vice to avoid potential soft areas of decalcification (none were found). We also avoided enamel immediately around cracks to avoid contamination with diagenetic minerals (see Sect "Discussion" for a detailed evaluation of diagenesis). For bulk samples, we aimed to maximize temporal averaging. Accordingly, we extracted 15–20 mg of clean enamel powder from a ca. 5 mm-wide band running from the cusp to cervical margin of an easily accessible surface of each tooth (Fig. 2). Conversely, for serial samples, we aimed to minimize temporal averaging and carved shallow grooves (ca. 1 mm wide by 0.5 mm deep) perpendicular to the growth axis of the tooth (Fig. 2). Groove centres were placed 3 mm apart, leaving ca. 2 mm gaps between each groove (Fig. 2). We collected serial samples from the M_2 talonid and M_3 trigonid, as they had the tallest exposed crowns. The basal groove was placed ca. 1 mm above the cervical margin, and we ensured the uppermost groove did not damage the occlusal surface. Grooves were elongated laterally until ca. 10 mg of enamel were collected.

Chemical pretreatment of powdered enamel followed Baumann and Crowley[76]. Samples were reacted with 30% hydrogen peroxide for 24 h at room temperature and rinsed five times with ultrapure water. Samples were agitated frequently while reacting, and tube lids were kept loose to allow evolved gas to escape. Next, samples were soaked in 1 M acetic acid buffered with calcium acetate for 24 h at 4 °C, again with frequent agitation. They were rinsed another five times with ultrapure water, and finally freeze dried.

Sample analysis

Bulk data for *T. major* M_3's (N = 13) were originally published in Ward et al.[29] The remaining samples (13 bulk-sampled M_2's and 92 serial samples) were analysed at the University of Florida's Light Stable Isotope Mass Spec Laboratory. Approximately 1 mg of sample was reacted with 100% phosphoric acid at 70 °C for 5 min in a Thermo Scientific Kiel II carbonate device and analysed with a Finnegan MAT 252 isotope ratio mass spectrometer. Both $\delta^{13}C$ and $\delta^{18}O$ data were calibrated to the Vienna PeeDee Belemnite (VPDB) scale using NBS 19. Analytical precision was monitored using repeated measurements of NBS 19 and NBS 18 (N = 48 and 13, respectively) and was ± 0.08‰ for carbon and ± 0.05‰ for oxygen (± 1 standard deviation). Accuracy, which was calculated using the difference between repeated measurements for NBS 18 and the known value for this standard ($\delta^{13}C_{VPDB}$: −5.014‰ ± 0.035‰; $\delta^{18}O_{VPDB}$: −23.2‰ ± 0.1‰), was ± 0.04‰ for carbon and ± 0.22‰ for oxygen. The total analytical uncertainty (determined using the calculator provided in Appendix G of Szpak et al.[77] and references therein) was ± 0.09‰ for carbon and ± 0.22‰ for oxygen. Completed calculators can be found in the online repository (https://github.com/clark-ward/2024SciRep).

Strontium analyses were performed at the Multicollector ICPMS Laboratory in the Department of Geology at the University of Illinois Urbana-Champaign. Approximately 6–8 mg of pre-treated powdered sample were dissolved in 0.5 mL of 3 M nitric acid. These solutions were filtered through Eichrom Sr-specific resin in Teflon mini-columns. Cations other than strontium were removed from the resin with 3 M and 8 M nitric acid. Strontium was then flushed from the resin with 4.0 mL of 0.05 M nitric acid into 4 mL autosampler vials. Strontium isotope ratios were analysed on a Nu Plasma high resolution multicollector inductively-coupled plasma mass spectrometer. International standard NBS 987 (known $^{87}Sr/^{86}Sr = 0.71026$) was used to calibrate $^{87}Sr/^{86}Sr$ throughout runs. Two internal carbonate standards, "Coral" ($^{87}Sr/^{86}Sr = 0.70918$) and "E&A" ($^{87}Sr/^{86}Sr = 0.70804$), were used to monitor and calculate accuracy and precision. Analytical precision was ± 0.00003 based on long-term replicates of both external and internal standards. To detect possible contamination or alteration, strontium concentrations were analysed for all serial samples (N = 92) on a Thermo Scientific iCAP Qc quadrupole inductively coupled plasma mass spectrometer. Precision of Sr concentration measurements was ca. 5% based on replicate measurements of 1:100 dilutions of SRM-1643f. (an acidified water standard). To calculate enamel Sr concentrations (μg Sr per g sample), we multiplied measured Sr concentrations by volume (4.0 mL) and divided by the mass of each analyzed sample.

Data analysis

Statistical analyses were conducted in R v.4.2.2[78] with the significance threshold (α) set to 0.05. Data and results were visualized using R and Inkscape 1.1. All code and data used in this study are provided online (https://github.com/clark-ward/2024SciRep). Because sample sizes were small, we used non-parametric statistical tests. To evaluate homogeneity of variance among groups, we used Fligner-Killeen tests (F-K; 'fligner.test' in 'stats' package[78]). We used unpaired Wilcoxon tests ('wilcox.test' in 'stats' with 'paired' argument set to false) to compare male and female *Teleoceras*, and paired Wilcoxon tests ('paired' set to true) to compare data for M_2's and M_3's from the same individuals. We also calculated the isotopic difference (Δ) between M_3 and M_2 (e.g., $\Delta\delta^{13}C_{M3\text{-}M2}$) for each individual, and we compared these Δ values for males and females using unpaired Wilcoxon tests. We accepted $\Delta^{87}Sr/^{86}Sr_{M3\text{-}M2}$ values greater than ± 0.00006 to be biologically meaningful; values less than this were attributed to analytical uncertainty.

Following Ward et al.[29], we statistically compared bulk $\delta^{13}C$, $\delta^{18}O$, and $^{87}Sr/^{86}Sr$ data for *Teleoceras* with co-occurring equids (including *Cormohipparion, Pliohippus, Pseudhipparion*), camelids (*Procamelus* and *Protolabis*), and a small hornless blastomerycine ruminant (*Longirostromeryx*). Here, we used a single isotopic value (averaging data for M_2 and M_3) for each *Teleoceras* individual in our comparison. We used Kruskal–Wallis tests (K-W; 'kruskal.test' in 'stats') to compare median isotopic values among families, followed by post-hoc Dwass-Steele-Critchlow-Fligner all-pairs tests (DSCF; 'dscfAllPairsTest' in 'PMCMRplus' package[79]). We also used F-K tests to assess variance homogeneity.

Lastly, we compared the overall variability in $^{87}Sr/^{86}Sr$ observed for *Teleoceras* bulk and serial samples, as well as all Ashfall ungulates, with estimated variability in bioavailable $^{87}Sr/^{86}Sr$. Our estimations were based on the isoscape by Reich et al.[75], which was built using modern published plant data and bedrock age models[43,80]. Using QGIS 3.22.9, we estimated the range of bioavailable $^{87}Sr/^{86}Sr$ within seven increasingly large areas centered on Ashfall (10, 50, 100, 500, 1,000, 5,000, and 10,000 km^2; Table 1). We acknowledge that sedimentary

Radius (km)	Area (km^2)	$^{87}Sr/^{86}Sr$ range
1.78	10	0.000108
3.99	50	0.000514
5.64	100	0.001230
12.62	500	0.001521
17.84	1000	0.001521
39.89	5000	0.002021
56.42	10,000	0.002648

Table 1. Estimated range in $^{87}Sr/^{86}Sr$ within increasingly large areas centered on Ashfall. Estimates are based on the modern bioavailable $^{87}Sr/^{86}Sr$ isoscape of eastern North America from Reich et al.[75] and were calculated using QGIS 3.22.9

rocks exposed in Nebraska today are different from those that were present in the mid-Miocene. In particular, modern sedimentary deposits are dominated by glacially derived loess and alluvium deposited during the Late Quaternary[75,80]. Consequently, regional bioavailable $^{87}Sr/^{86}Sr$ has likely changed since the Miocene. Nevertheless, the modern isoscape should provide a reasonable rough estimate of the potential range in bioavailable $^{87}Sr/^{86}Sr$ during the Miocene.

Results

Overall, $\delta^{13}C$ values for bulk *Teleoceras* enamel ranged from −9.6 to −7.7‰ (−8.5 ± 0.5‰; mean and one standard deviation), $\delta^{18}O$ values ranged from −7.8 to −4.8‰ (−6.3 ± 0.8‰), and $^{87}Sr/^{86}Sr$ ranged from 0.70863 to 0.70874 (0.70868 ± 0.00003; Fig. 3; Table 2a; Supplementary Table S1). There was considerable overlap between males and females, and between M_2's and M_3's of each sex for all three isotopes (Fig. 3; Table 2a; Supplementary Table S1). We found only one significant difference: median $\delta^{13}C$ values for female M_2's were ca. 0.5‰ lower than for female M_3's (Fig. 3; Table 2a). Isotopic variances were not significantly different between sexes or tooth positions for any isotope (F-K $p > 0.05$; Table 2a). Medians and isotopic variances of the isotopic difference between M_2's and M_3's (Δ) were also statistically indistinguishable between sexes for all isotopes (Fig. 3; Table 2b). Combining data for both sexes, $\Delta\delta^{13}C_{M3\text{-}M2}$ ranged from −0.6 to 1.0‰ (0.2 ± 0.4‰), $\Delta\delta^{18}O_{M3\text{-}M2}$ ranged from −1.4 to 2.4‰ (0.2 ± 1.2‰), and $\Delta^{87}Sr/^{86}Sr_{M3\text{-}M2}$ ranged from −0.00004 to 0.00005 (0.00000 ± 0.00003; Fig. 3; Table 2b).

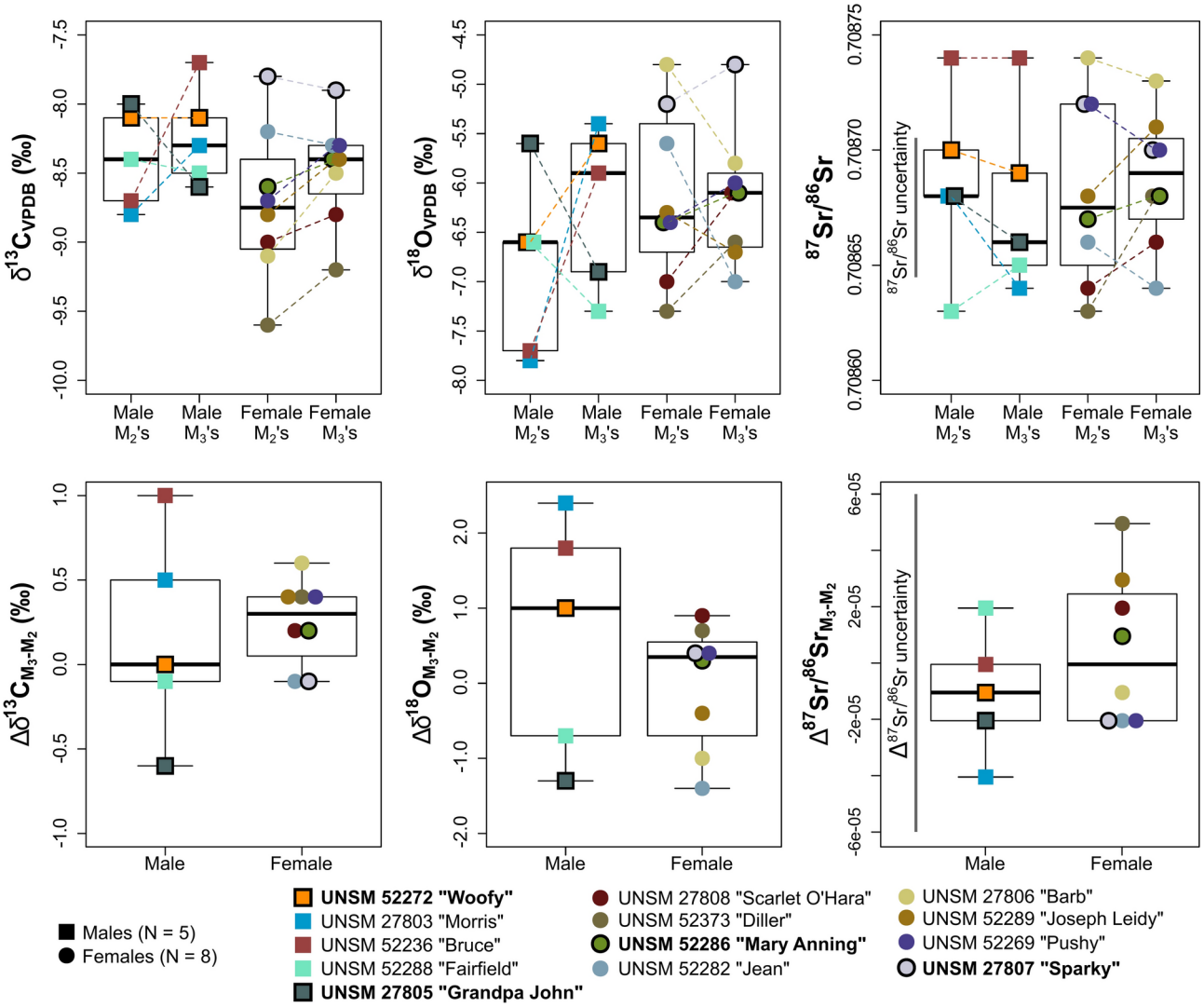

Fig. 3. Box plots showing $\delta^{13}C$, $\delta^{18}O$, and $^{87}Sr/^{86}Sr$ data for bulk sampled male and female *Teleoceras major* M_2's and M_3's (upper panel), and the isotopic difference (Δ) between M_3's and M_2's for each individual (lower panel). Summary statistics are provided in Table 2. Box midlines represent medians. Lower and upper box boundaries are the 25th and 75th percentiles, respectively, and whisker lines designate total ranges. Dashed lines connect M_2 and M_3 data from the same individual. Data for individuals that were also serially sampled (Woofy, Grandpa John, Mary Anning, and Sparky) are outlined in black. Gray solid bars labelled "$^{87}Sr/^{86}Sr$ uncertainty" and "$\Delta^{87}Sr/^{86}Sr$ uncertainty" illustrate analytical uncertainty (± 0.00003 and ± 0.00006, respectively). M_3 data from Ward et al.[29].

(A) Sex	Element	N	$\delta^{13}C_{VPDB}$ (‰)		$\delta^{18}O_{VPDB}$ (‰)		$^{87}Sr/^{86}Sr$	
			Mean ± 1σ	Median	Mean ± 1σ	Median	Mean ± 1σ (× 10^{-5})	Median
Male	M_2	5	−8.4 ± 0.4	−8.4	−6.9 ± 0.9	−6.6	0.70869 ± 4.0	0.70868
Male	M_3	5	−8.2 ± 0.4	−8.3	−6.2 ± 0.8	−5.9	0.70868 ± 4.0	0.70866
Female	M_2	8	−8.7 ± 0.6	−8.8	−6.1 ± 0.9	−6.4	0.70868 ± 4.0	0.70868
Female	M_3	8	−8.5 ± 0.4	−8.4	−6.1 ± 0.7	−6.1	0.70869 ± 2.9	0.70869
Male M_2 vs. M_3:			Unpaired Wilcoxon:	V = 4; $p = 0.86$		V = 4; $p = 0.44$		V = 7.5; $p = 0.46$
			F-K:	$\chi^2 = 0.26$; $p = 0.61$		$\chi^2 = 0.004$; $p = 0.95$		$\chi^2 = 0.03$; $p = 0.87$
Female M_2 vs. M_3:			Unpaired Wilcoxon:	V = 3; $p =$ **0.042**		V = 18; $p = 1$		V = 16.5; $p = 0.7$
			F-K:	$\chi^2 = 1.29$; $p = 0.26$		$\chi^2 = 0.80$; $p = 0.37$		$\chi^2 = 0.77$; $p = 0.38$
M_2 Male vs. Female:			Paired Wilcoxon:	W = 28; $p = 0.27$		W = 9.5; $p = 0.14$		W = 22; $p = 0.82$
			F-K:	$\chi^2 = 0.29$; $p = 0.59$		$\chi^2 = 0.009$; $p = 0.93$		$\chi^2 = 0.08$; $p = 0.77$
M_3 Male vs. Female:			Paired Wilcoxon:	W = 26; $p = 0.46$		W = 21; $p = 0.94$		W = 15; $p = 0.51$
			F-K:	$\chi^2 = 0.06$; $p = 0.80$		$\chi^2 = 0.62$; $p = 0.43$		$\chi^2 = 0.009$; $p = 0.93$
(B) Sex	Element	N	$\Delta\delta^{13}C_{M3\text{-}M2\ VPDB}$ (‰)		$\Delta\delta^{18}O_{M3\text{-}M2\ VPDB}$ (‰)		$\Delta\delta^{87}Sr/^{86}Sr_{M3\text{-}M2}$	
			Mean ± 1σ	Median	Mean ± 1σ	Median	Mean ± 1σ (× 10^{-5})	Median
Male	$M_{3\text{-}2}$	5	0.2 ± 0.6	0.0	0.6 ± 1.6	1.0	−0.00001 ± 2.2	−0.00001
Female	$M_{3\text{-}2}$	8	0.3 ± 0.3	0.3	−0.1 ± 0.8	0.4	0.00001 ± 2.7	0.00000
Male vs. Female:			Paired Wilcoxon:	W = 19; $p = 0.94$		W = 27; $p = 0.34$		W = 15; $p = 0.51$
			F-K:	$\chi^2 = 1.51$; $p = 0.22$		$\chi^2 = 1.70$; $p = 0.19$		$\chi^2 = 0.72$; $p = 0.40$

Table 2. Summary descriptive statistics and Wilcoxon and Fligner–Killeen (F-K) test results for (A) bulk-sampled *Teleoceras major* M_2's and M_3's and (B) the isotopic difference (Δ) between bulk sampled *Teleoceras major* M_3's and M_2's. Significant results are in bold. All F-K tests had one degree of freedom. All $\Delta^{87}Sr/^{86}Sr$ values were within analytical uncertainty (± 0.00006), see Methods and Fig. 3

UNSM no	Name	Sex	Element	No. of grooves	$\delta^{13}C_{VPDB}$ (‰)			$\delta^{18}O_{VPDB}$ (‰)			$^{87}Sr/^{86}Sr$		
					Max	Min	Range	Max	Min	Range	Max	Min	Range
52247	Woofy	M	M_2	11	−8.0	−8.5	0.5	−5.0	−7.0	2.0	0.70870	0.70866	0.00004
52247	Woofy	M	M_3	10	−8.1	−8.6	0.5	−5.2	−7.5	2.3	0.70870	0.70866	0.00004
27805	Grandpa John	M	M_2	12	−8.9	−9.8	0.9	−3.9	−7.7	3.8	0.70871	0.70867	0.00004
27805	Grandpa John	M	M_3	14	−8.4	−9.5	1.1	−5.0	−8.1	3.1	0.70868	0.70862	0.00006
52286	Mary Anning	F	M_2	9	−8.4	−9.7	1.3	−4.0	−6.8	2.8	0.70867	0.70861[a]	0.00006[a]
52286	Mary Anning	F	M_3	10	−9.2	−10.0	0.8	−4.8	−7.8	3.0	0.70869	0.70864	0.00005
27807	Sparky	F	M_2	13	−8.0	−9.4	1.4	−4.1	−7.5	3.4	0.70875	0.70868	0.00007
27807	Sparky	F	M_3	13	−7.9	−8.6	0.7	−5.4	−7.5	2.1	0.70874	0.70869	0.00005

Table 3. Summary statistics for serially sampled *Teleoceras major* molars from Ashfall. Most of the variability in $^{87}Sr/^{86}Sr$ was within analytical uncertainty (± 0.00003). [a]The basal-most $^{87}Sr/^{86}Sr$ datum for Mary Anning's M_2 was an outlier (= 0.70856). This $^{87}Sr/^{86}Sr$ datum was excluded from these calculations; see Sect "Results" for details.

Isotopic ranges for serially sampled teeth for each *Teleoceras* individual are summarized in Table 3 and details are provided in Fig. 4 and Supplementary Table S2. We found low variability in $\delta^{13}C$ values (< 1.5‰) for all serially sampled molars. In contrast, $\delta^{18}O$ values fluctuated by 2–4‰ for all teeth (Fig. 4; Table 3). Strontium isotope ratios were within analytical uncertainty (± 0.00003) with two exceptions: the M_2 for Sparky (UNSM 27807) had an overall range of 0.00007, and the basal-most sample for the M_2 of Mary Anning (UNSM 52286) had an anomalously low ratio (0.70856) (Fig. 4; Table 3). The slightly elevated range in $^{87}Sr/^{86}Sr$ for Sparky's M_2 was not driven by a single outlier, nor did any of the serial samples have an unusual Sr concentration (Fig. 3; Supplementary Table S2). In contrast, the sample for Mary Anning also had an anomalously high Sr concentration of 900.67 µg Sr per g sample (compared to 257.83–629.11 µg Sr per g sample for all other serial samples; Supplementary Table S2). We therefore excluded the $^{87}Sr/^{86}Sr$ datum for this sample from summary statistics and intertooth comparisons.

There were some visible differences among serially sampled individuals. For example, $\delta^{13}C$ values were non-overlapping for Grandpa John and Woofy's M_2's, and Mary Anning and Sparky's M_3's (Fig. 5a). Both M_2 and M_3 for Mary Anning and Sparky had apparently distinct ranges in $^{87}Sr/^{86}Sr$, but these were all within analytical uncertainty (Fig. 5c). Oxygen isotope values were overlapping among all serially sampled molars (Fig. 5b). Overall, isotopic data for serial sampled teeth were isotopically comparable to bulk data (Fig. 5).

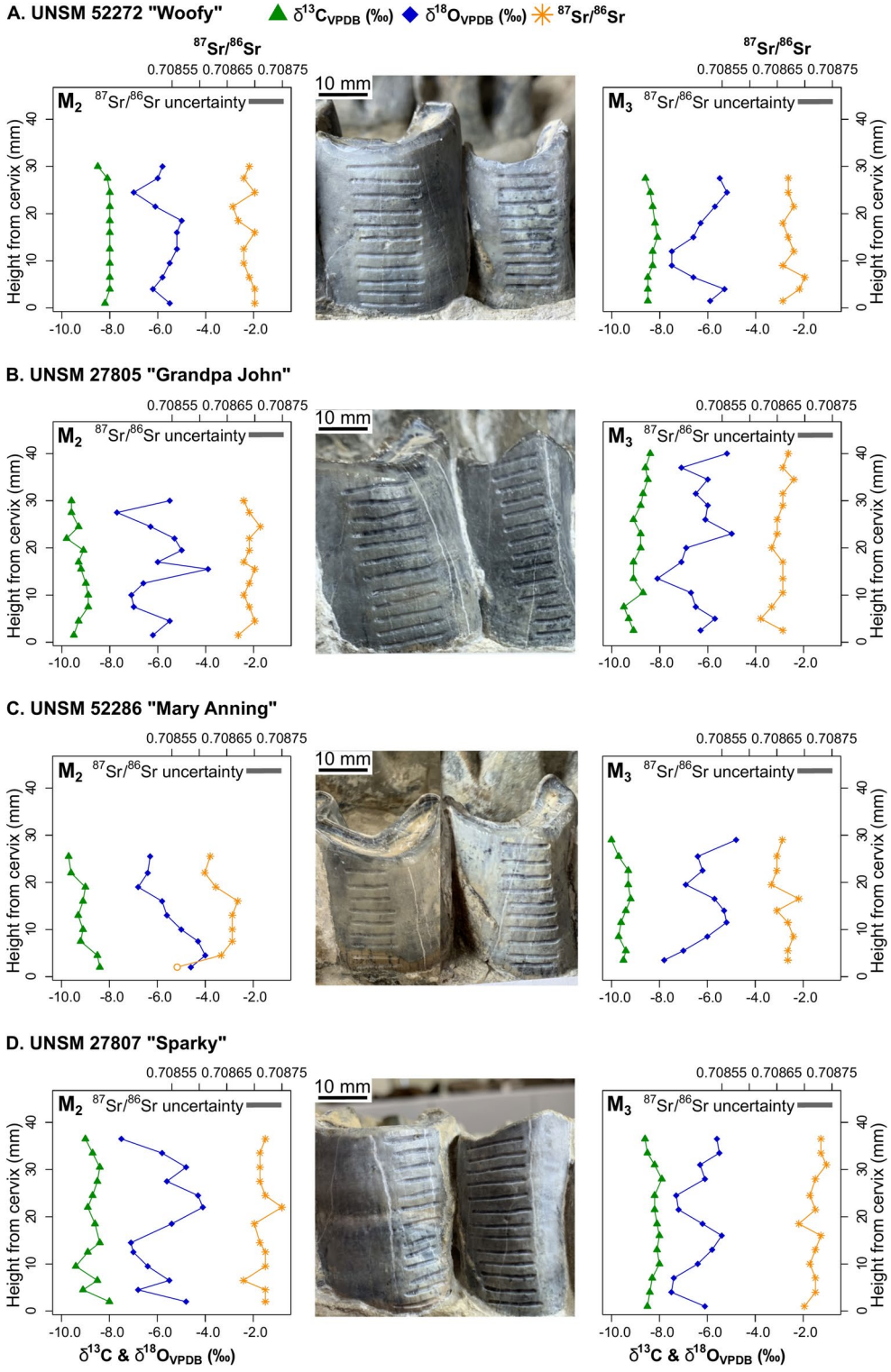

Fig. 4. Isotopic results for serially sampled molars from male (panels A and B) and female (panels C and D) *Teleoceras major* at Ashfall. Summary data (minima, maxima, and ranges) are provided in Table 3. The basal-most $^{87}Sr/^{86}Sr$ datum for Mary Anning's M_2 (open circle) is a statistical outlier and was excluded from analyses. Gray solid bar labelled "$^{87}Sr/^{86}Sr$ uncertainty" indicates analytical uncertainty (± 0.00003). Photographs by CTW, used with permission from the University of Nebraska State Museum.

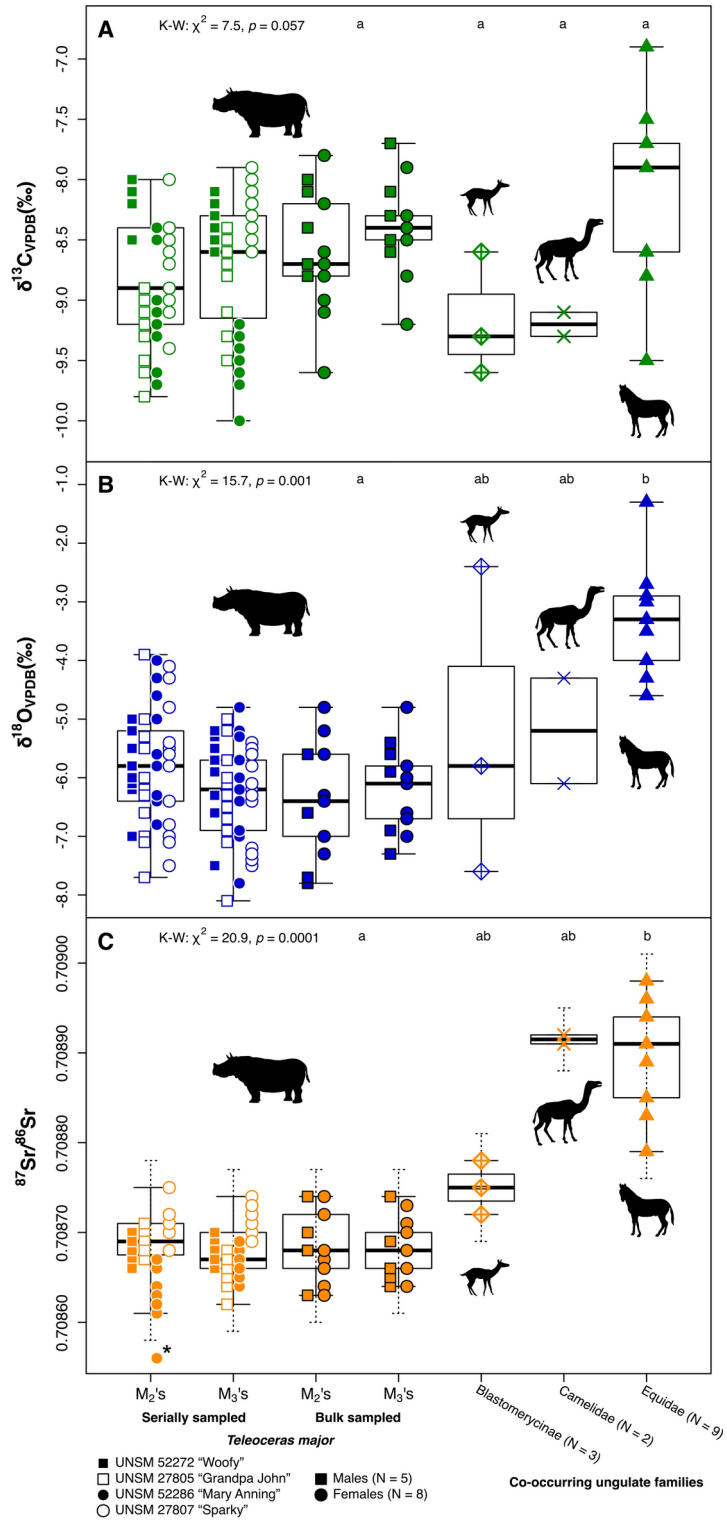

Similar to Ward et al.[29], we found that $\delta^{13}C$ was statistically indistinguishable among ungulate families (Fig. 5a). In contrast, median $\delta^{18}O$ and $^{87}Sr/^{86}Sr$ differed significantly among families (Fig. 5b, c). Post hoc DSCF tests indicate that Equidae had significantly higher $\delta^{18}O$ and $^{87}Sr/^{86}Sr$ medians than Rhinocerotidae while Camelidae and Blastomerycinae were statistically indistinguishable from other families (Fig. 5c; Supplementary Table S3). Finally, the observed range in $^{87}Sr/^{86}Sr$ for all bulk and serial *T. major* data (0.00016; 0.00020 when accounting for analytical uncertainty) was larger than the estimated range of biologically available $^{87}Sr/^{86}Sr$ within a circular area of 10 km^2 (0.000108), but considerably smaller than the estimated range for 50 km^2 (0.000514; Table 1). The total range in $^{87}Sr/^{86}Sr$ for all ungulates (0.00037; 0.00043 with uncertainty) was also smaller than the estimated isotopic range for 50 km^2 (Table 1).

◀**Fig. 5**. Box plots displaying isotopic ranges for serial and bulk sampled *Teleoceras major* molars, as well as previously published bulk sampled teeth from co-occurring ungulate families at Ashfall (from Ward et al.[29]). Blastomerycinae included data from one genus, *Longirostromeryx* (N = 3), Camelidae included two genera, *Procamelus* (N = 1) and *Protolabis* (N = 1), and Equidae included three genera, *Pseudhipparion* (N = 3), *Pliohippus* (N = 3), and *Cormohipparion* (N = 3). We used a single isotopic value (averaging bulk M_2 and M_3 data) for each *Teleoceras* individual in our comparison. Box midlines represent medians, the lower and upper box boundaries are the 25th and 75th percentiles, respectively, and solid whisker lines designate the total range of data. Dotted lines in panel C account for analytical uncertainty (± 0.00003). Families that share a lowercase letter were statistically indistinguishable based on post-hoc Dwass–Steele–Critchlow–Fligner all-pairs tests. The $^{87}Sr/^{86}Sr$ datum with an asterisk was an outlier for Mary Anning's M_2 and was excluded from all statistical analyses (see Sect "Results" for details). Silhouettes are not to scale and are based off paintings by Mark Marcuson, used with permission from the University of Nebraska State Museum.

Discussion

We set out to evaluate the mobility of *Teleoceras major* at Ashfall Fossil Beds. Sexual dimorphism and the associated inferred mating system of *Teleoceras* both suggest male-biased natal dispersal. However, we found no evidence for natal dispersal, seasonal migration, or long-distance movement. Both bulk and serial isotopic data are consistent with *T. major* at Ashfall having had limited mobility throughout life.

Bulk isotopic data suggest no differences in foraging ecology or landscape use before and after cow-calf separation for males or females (Fig. 3; Table 2). Carbon isotope values were slightly (ca. 0.5‰) lower for female M_2's than female M_3's, but this shift was inconsistent in direction and magnitude among individuals (Fig. 3; Table 2a) and too small to be ecologically meaningful[28]. Similarly, $\Delta\delta^{13}C_{M3\text{-}M2}$ and $\Delta\delta^{18}O_{M3\text{-}M2}$ ranges were all small (1.6‰ and 3.8‰, respectively), and all $\Delta^{87}Sr/^{86}Sr_{M3\text{-}M2}$ were within analytical uncertainty (Fig. 3; Table 2b). These results further indicate that none of the sampled individuals immigrated to Ashfall after M_3 formation, either due to dispersal later in life or while seeking refugium from ash.

Serial data provide additional support for low mobility (Fig. 4). Minimally variable $\delta^{13}C$ (< 1.5‰) and $^{87}Sr/^{86}Sr$ ranges within or close to analytical uncertainty suggest that all sampled *T. major* individuals had a consistent diet of C_3 plants and foraged in the same area year-round before and after cow-calf separation (Fig. 4; Table 3). Small intra-annual variability in $\delta^{13}C$ values is expected for animals that solely consume C_3 vegetation[28], and has also been observed in serially-sampled tusks from the browsing proboscidean *Gomphotherium* sp. from Clarendonian Nebraska[30]. The observed oscillations in $\delta^{18}O$ values of 2–4‰ within individual serially sampled *T. major* teeth (Fig. 4; Table 3) are consistent with seasonal differences in precipitation rather than changes in diet or geography, particularly when paired with lowly variable $\delta^{13}C$ and $^{87}Sr/^{86}Sr$[17,38,39,81]. Homogeneous $^{87}Sr/^{86}Sr$ ranges (i.e., close to or within analytical uncertainty of ± 0.00003) for both bulk and serial sampled *T. major* molars therefore cannot exclude short-term or short-distance movements, but also do not support sustained long-distance movement.

We are confident that our data are biological, and that low isotopic variability cannot be explained by diagenetic alteration or time averaging due to bimodal timing of enamel crystallization. Previous studies[29,41] have shown that Ashfall specimens retain biogenic isotopic signals with no detectable diagenetic alteration. With the exception of the basal-most sample for Mary Anning's M_2, Sr concentration ranged between 257.83 and 629.11 µg Sr per g sample (Supplementary Table S2), which is consistent with previously published concentrations for other modern, Pleistocene, and Miocene large ungulates and proboscideans[82,83]. We suspect the anomalous serial sample from Mary Anning's M_2 was the result of contamination rather than diagenetic alteration (or evidence for mobility), as $\delta^{13}C$ and $\delta^{18}O$ values were consistent with other samples from that tooth. Ward et al.[29] previously found small—but statistically distinct—isotopic differences among co-occurring ungulate taxa at Ashfall when only *Teleoceras* M_3's were included, and we observed similar patterns when data for *Teleoceras* M_2's were incorporated as average values (Fig. 5). Variable $\delta^{18}O$ values within serially sampled teeth, as well as apparent (but negligible) $^{87}Sr/^{86}Sr$ and distinct $\delta^{13}C$ ranges among some serially sampled individuals further suggest that the data are biogenic.

During enamel formation, crystals are mineralized during two separate phases, which are averaged together during isotopic sampling[71,74]. Consequently, serial isotopic data do not represent instantaneous points in time and patterns in serial isotopic data are dampened compared to inputs from the body[73,74]. This dampening is particularly pronounced for $^{87}Sr/^{86}Sr$ in enamel due to slow turnover of Sr within the body[74,84]. Nevertheless, enamel $^{87}Sr/^{86}Sr$ would still be expected to vary for a species that undergoes long distance movement (e.g., Caribou, *Rangifer tarandus* and American Bison, *Bison bison*), even when using a conventional sampling strategy like the one we employed[53,85].

We acknowledge that we sampled a relatively small number of individuals, and it is thus possible immigrants may have gone undetected. Moreover, if *Teleoceras major* formed groups (which we think is likely), it is also possible that we only sampled members of the same group. All of the individuals we were able to sample (which includes all of the available male specimens of *T. major* in the UNSM collections) were buried close together (see map of skeletons in ref.[21]). We also would not be able to detect emigrants, as they would not have been buried in the ash bed. However, if immigration was as common as emigration, then we would expect to find isotopic evidence for immigration, which is not the case (Fig. 5).

We note that *Longirostromeryx*, which was the smallest ungulate at Ashfall (ca. 15 kg) and therefore the most likely to have been local to the Ashfall area[86], had statistically indistinguishable $\delta^{13}C$, $\delta^{18}O$, and $^{87}Sr/^{86}Sr$ from all other ungulate families at Ashfall, including Rhinocerotidae (Fig. 5). This either suggests that all sampled individuals were local, or that the region was isotopically homogenous. Compared to the modern $^{87}Sr/^{86}Sr$

isoscape of Reich et al.[75], the range in $^{87}Sr/^{86}Sr$ observed for both *Teleoceras major* and ungulates overall is larger than the estimated range in modern bioavailable $^{87}Sr/^{86}Sr$ within a 10 km^2 area from Ashfall, but smaller than an area of 50 km^2 (Table 1). This comparison suggests that the region was not isotopically homogeneous and that all sampled individuals were local to Ashfall prior to death. Distinctly different $\delta^{18}O$ and $^{87}Sr/^{86}Sr$ medians between *T. major* and co-occurring horses (Fig. 5b, c) further support local isotopic variability. Ward et al.[29] previously argued that small (but significant) isotopic differences between horses and *T. major* reflect differences in preferred foraging habitat with *T. major* having a semi-aquatic lifestyle and favouring wet habitats. A semi-aquatic lifestyle likely would have prohibited long-distance movement across multiple habitats. Like the extant common hippopotamus, *T. major* would have had a limited foraging range, as the physiological requirement to submerge in water tethers an individual to standing bodies of water[87].

It is possible that *Teleoceras major* was able to avoid moving seasonally by switching its diet to more herbaceous or woody vegetation when C_3 grasses were not available[10,11]. It is also possible that the moist habitats preferred by *T. major*, or alternatively a warm equable climate, supported sufficient forage for *T. major* year-round, such that diet-switching was unnecessary. Migration is suggested to have originated among extant ungulates during the middle–late Miocene in association with drying, cooling, and increased seasonality of central North America[11,16,17,88]; seasonal migratory behaviour may not yet have evolved when the Ashfall ungulates were alive. Increased primary productivity, due to a more equable Miocene climate, may have bolstered resource availability and ungulate biomass[4,16]. Additionally, as observed in modern ecosystems, nutrient cycling can be enhanced by large herbivores and lead to increased herbivore biomass[89,90]. This could have also influenced productivity in the mid-Miocene.

With limited mobility, *Teleoceras major* likely had adaptations to avoid inbreeding. For example, individuals could have socially dispersed among groups[91,92]. Female modern white rhinoceroses (*Ceratotherium simum*) have been observed to select mates that are genetically different[93], and *T. major* may have had a similar adaptation to avoid inbreeding when neither sex spatially dispersed. All modern rhinoceroses frequently use mud wallows to protect their skin from parasites and the sun and to thermoregulate[63,94]. Mud wallows also contribute to rhinoceros sociality by catalysing direct interactions and indirect communications like scent marking[63,94]. Thus, a preference for wet habitats with standing water and mud may have been tied to the behaviour, physiology, sociality, and thermoregulation of *T. major*.

Finally, it is conceivable that the *Teleoceras major* individuals buried at Ashfall moved along an isotopically homogeneous riparian corridor with similar vegetation, moisture, and soils. Homogeneous $^{87}Sr/^{86}Sr$ ranges (i.e., close to or within analytical uncertainty of ± 0.00003) for both bulk and serial sampled *T. major* molars do not support sustained long-distance movement but cannot exclude short-term or short-distance movements. Modern common hippopotamuses congregate in dense, large groups during the dry season and spread out again during the wet season, yet they stay within the same water system[87], and *T. major* may have behaved similarly. The geomorphological origin of the watering-hole at Ashfall is unknown[21,59], but it could have been part of a series of watering-holes or oxbow lakes associated with a large meandering stream. The silty sandstones underlying the Ashfall ash bed were interpreted as floodplain deposits, but these rocks are poorly exposed elsewhere and evidence for a laterally expansive channel system is lacking[21,59].

Conclusions

We set out to investigate three types of potential mobility in *Teleoceras major* at Ashfall Fossil Beds: (1) natal dispersal, (2) seasonal migration, and (3) response to catastrophic volcanic eruption. Unexpectedly, we found strong evidence for a relatively sedentary lifestyle and a lack of any long-distance movement. A warm equable climate during the mid-Miocene may have resulted in high primary productivity and allowed large populations of ungulates to occupy the same area year-round. We further suggest that a semi-aquatic lifestyle may have required continuous access to water and limited *T. major* mobility. We propose that *T. major* may have utilized social, rather than spatial, dispersal among groups of individuals, although it is also possible that individuals moved short distances among watering-holes or oxbow lakes associated with a large meandering stream.

This is one of the first studies to use strontium isotope data to investigate migration and dispersal of a North American extinct species prior to the Quaternary. While we acknowledge the limitations and assumptions of applying modern isotopic methods to ancient landscapes, this study highlights how a multi-isotope approach can reveal unexpected behaviour in an extinct organism. In particular, the inclusion of strontium isotopes provides nuanced spatial information that complements more widely used carbon and oxygen isotopes, even in a geologically homogenous setting. Future research reconstructing Miocene ungulate mobility could yield additional insight into movement patterns prior to the global expansion of C_4 grassy biomes.

Data availability

All data generated and analysed during this study are included in this published article, its Supplementary Tables file, and the online repository (https://github.com/clark-ward/2024SciRep).

Received: 20 June 2024; Accepted: 11 March 2025
Published online: 04 April 2025

References

1. Staver, A. C., Abraham, J. O., Hempson, G. P., Karp, A. T. & Faith, J. T. The past, present, and future of herbivore impacts on savanna vegetation. *J. Ecol.* **109**, 2804–2822 (2021).
2. Pringle, R. M. et al. Impacts of large herbivores on terrestrial ecosystems. *Curr. Biol.* **33**, R584–R610 (2023).
3. Trepel, J. et al. Meta-analysis shows that wild large herbivores shape ecosystem properties and promote spatial heterogeneity. *Nat. Ecol. Evol.* **8**, 705–716 (2024).

4. Janis, C., Damuth, J. & Theodor, J. M. The species richness of Miocene browsers, and implications for habitat type and primary productivity in the North American grassland biome. *Palaeogeogr. Palaeoclimatol. Palaeoecol.* **207**, 371–398 (2004).
5. Janis, C. M., Damuth, J. & Theodor, J. M. Miocene ungulates and terrestrial primary productivity: where have all the browsers gone?. *Proc. Natl. Acad. Sci.* **97**, 7899–7904 (2000).
6. Morales-García, N. M., Säilä, L. K. & Janis, C. M. The Neogene savannas of North America: a retrospective analysis on artiodactyl faunas. *Front. Earth Sci.* **8**, 24 (2020).
7. Greenwood, P. J. Mating systems, philopatry and dispersal in birds and mammals. *Anim. Behav.* **28**, 1140–1162 (1980).
8. Dobson, F. S. Competition for mates and predominant juvenile male dispersal in mammals. *Anim. Behav.* **30**, 1183–1192 (1982).
9. Lawson Handley, L. J. & Perrin, N. Advances in our understanding of mammalian sex-biased dispersal. *Mol. Ecol.* **16**, 1559–1578 (2007).
10. Abraham, J. O., Hempson, G. P., Faith, J. T. & Staver, A. C. Seasonal strategies differ between tropical and extratropical herbivores. *J. Anim. Ecol.* **91**, 681–692 (2022).
11. Abraham, J. O., Upham, N. S., Damian-Serrano, A. & Jesmer, B. R. Evolutionary causes and consequences of ungulate migration. *Nat. Ecol. Evol.* **6**, 998–1006 (2022).
12. Aikens, E. O. et al. Wave-like patterns of plant phenology determine ungulate movement tactics. *Curr. Biol.* **30**, 3444-3449.e4 (2020).
13. Ehleringer, J. R. & Dawson, T. E. Water uptake by plants: perspectives from stable isotope composition. *Plant Cell Environ.* **15**, 1073–1082 (1992).
14. Archibald, S. & Scholes, R. J. Leaf green-up in a semi-arid African savanna -separating tree and grass responses to environmental cues. *J. Veg. Sci.* **18**, 583–594 (2007).
15. Owen-Smith, R. N. *Megaherbivores: The Influence of Very Large Body Size on Ecology* (Cambridge University Press, 1988).
16. Fox, D. L. & Koch, P. L. Carbon and oxygen isotopic variability in Neogene paleosol carbonates: constraints on the evolution of the C4-grasslands of the Great Plains, USA. *Palaeogeogr. Palaeoclimatol. Palaeoecol.* **207**, 305–329 (2004).
17. Kukla, T. et al. Drier winters drove Cenozoic open habitat expansion in North America. *AGU Adv.* **3**, e2021AV000566 (2022).
18. Abraham, J. O., Hempson, G. P. & Staver, A. C. Drought-response strategies of savanna herbivores. *Ecol. Evol.* **9**, 7047–7056 (2019).
19. Walker, R. H. et al. Trait-based sensitivity of large mammals to a catastrophic tropical cyclone. *Nature* **623**, 757–764 (2023).
20. Smith, J. J., Turner, E., Möller, A., Joeckel, R. M. & Otto, R. E. First U-Pb zircon ages for late Miocene Ashfall Konservat-Lagerstätte and Grove Lake ashes from eastern Great Plains, USA. *PLoS One* **13**, e0207103 (2018).
21. Tucker ST, Otto RE, Joeckel RM, Voorhies MR. The geology and paleontology of Ashfall Fossil Beds, a late Miocene (Clarendonian) mass-death assemblage, Antelope County and adjacent Knox County, Nebraska, USA. In *Geologic Field Trips along the Boundary between the Central Lowlands and Great Plains: 2014 Meeting of the GSA North-Central Section.* Geological Society of America, 1–22. (2014).
22. Perkins, M. E. & Nash, B. P. Explosive silicic volcanism of the Yellowstone hotspot: the ash fall tuff record. *Geol. Soc. Am. Bull.* **114**, 367–381 (2002).
23. Cerling, T. E., Harris, J. M. & Passey, B. H. Diets of east African Bovidae based on stable isotope analysis. *J. Mammal.* **84**, 456–470 (2003).
24. Sponheimer, M. et al. Diets of southern African Bovidae: stable isotope evidence. *J. Mammal.* **84**, 471–479 (2003).
25. Fox, D. L. & Koch, P. L. Tertiary history of C_4 biomass in the Great Plains, USA. *Geology* **31**, 809–812 (2003).
26. Nguy, W. H. & Secord, R. Middle Miocene paleoenvironmental reconstruction in the central Great Plains, USA, from stable carbon isotopes in ungulates. *Palaeogeogr. Palaeoclimatol. Palaeoecol.* **594**, 110929 (2022).
27. Kita, Z. A., Secord, R. & Boardman, G. S. A new stable isotope record of Neogene paleoenvironments and mammalian paleoecologies in the western Great Plains during the expansion of C_4 grasslands. *Palaeogeogr. Palaeoclimatol. Palaeoecol.* **399**, 160–172 (2014).
28. Heaton, T. H. E. Spatial, species, and temporal variations in the $^{13}C/^{12}C$ ratios of C_3 plants: Implications for palaeodiet studies. *J. Archaeol. Sci.* **26**, 637–649 (1999).
29. Ward, C. T., Crowley, B. E. & Secord, R. Home on the range: A multi-isotope investigation of ungulate resource partitioning at Ashfall Fossil Beds, Nebraska, USA. *Palaeogeogr. Palaeoclimatol. Palaeoecol.* **650**, 112375 (2024).
30. Fox, D. L. & Fisher, D. C. Dietary reconstruction of Miocene *Gomphotherium* (Mammalia, Proboscidea) from the Great Plains region, USA, based on the carbon isotope composition of tusk and molar enamel. *Palaeogeogr. Palaeoclimatol. Palaeoecol.* **206**, 311–335 (2004).
31. Kohn, M. J. Predicting animal $\delta^{18}O$: Accounting for diet and physiological adaptation. *Geochim. Cosmochim. Acta* **60**, 4811–4829 (1996).
32. Bryant, J. D. & Froelich, P. N. A model of oxygen isotope fractionation in body water of large mammals. *Geochim. Cosmochim. Acta* **59**, 4523–4537 (1995).
33. Gat, J. R. Oxygen and hydrogen isotopes in the hydrologic cycle. *Annu. Rev. Earth Planet. Sci.* **24**, 225–262 (1996).
34. Farquhar, G. D., Cernusak, L. A. & Barnes, B. Heavy water fractionation during transpiration. *Plant Physiol.* **143**, 11–18 (2007).
35. Barbour, M. M. Stable oxygen isotope composition of plant tissue: a review. *Funct. Plant Biol.* **34**, 83 (2007).
36. Faith, J. T. Paleodietary change and its implications for aridity indices derived from $\delta^{18}O$ of herbivore tooth enamel. *Palaeogeogr. Palaeoclimatol. Palaeoecol.* **490**, 571–578 (2018).
37. Cerling, T. E. et al. Stable isotope ecology of the common hippopotamus. *J. Zool.* **276**, 204–212 (2008).
38. Trayler, R. B. & Kohn, M. J. Tooth enamel maturation reequilibrates oxygen isotope compositions and supports simple sampling methods. *Geochim. Cosmochim. Acta* **198**, 32–47 (2017).
39. Nelson, S. V. Paleoseasonality inferred from equid teeth and intra-tooth isotopic variability. *Palaeogeogr. Palaeoclimatol. Palaeoecol.* **222**, 122–144 (2005).
40. Levin, N. E., Cerling, T. E., Passey, B. H., Harris, J. M. & Ehleringer, J. R. A stable isotope aridity index for terrestrial environments. *Proc. Natl. Acad. Sci.* **103**, 11201–11205 (2006).
41. Clementz, M. T., Holroyd, P. A. & Koch, P. L. Identifying aquatic habits of herbivorous mammals through stable isotope analysis. *PALAIOS* **23**, 574–585 (2008).
42. Capo, R. C., Stewart, B. W. & Chadwick, O. A. Strontium isotopes as tracers of ecosystem processes: theory and methods. *Geoderma* **82**, 197–225 (1998).
43. Bataille, C. P. & Bowen, G. J. Mapping $^{87}Sr/^{86}Sr$ variations in bedrock and water for large scale provenance studies. *Chem. Geol.* **304–305**, 39–52 (2012).
44. Graustein, W. C. & Armstrong, R. L. The use of strontium-87/strontium-86 ratios to measure atmospheric transport into forested watersheds. *Science* **219**, 289–292 (1983).
45. Reynolds, A. C., Quade, J. & Betancourt, J. L. Strontium isotopes and nutrient sourcing in a semi-arid woodland. *Geoderma* **189–190**, 574–584 (2012).
46. Wallace, J. P., Crowley, B. E. & Miller, J. H. Investigating equid mobility in Miocene Florida, USA using strontium isotope ratios. *Palaeogeogr. Palaeoclimatol. Palaeoecol.* **516**, 232–243 (2019).
47. Hedman, K. M., Curry, B. B., Johnson, T. M., Fullagar, P. D. & Emerson, T. E. Variation in strontium isotope ratios of archaeological fauna in the Midwestern United States: a preliminary study. *J. Archaeol. Sci.* **36**, 64–73 (2009).

48. Esker, D., Forman, S. L., Widga, C., Walker, J. D. & Andrew, J. E. Home range of the Columbian mammoths (*Mammuthus columbi*) and grazing herbivores from the Waco Mammoth National Monument, (Texas, USA) based on strontium isotope ratios from tooth enamel bioapatite. *Palaeogeogr. Palaeoclimatol. Palaeoecol.* **534**, 109291 (2019).
49. Radloff, F. G. T., Mucina, L., Bond, W. J. & le Roux, P. J. Strontium isotope analyses of large herbivore habitat use in the Cape Fynbos region of South Africa. *Oecologia* **164**, 567–578 (2010).
50. Hamilton, M. I., Fernandez, D. P. & Nelson, S. V. Using strontium isotopes to determine philopatry and dispersal in primates: a case study from Kibale National Park. *R. Soc. Open Sci.* **8**, 200760 (2021).
51. Tütken, T. & Vennemann, T. Stable isotope ecology of Miocene large mammals from Sandelzhausen, southern Germany. *Paläontol. Z.* **83**, 207–226 (2009).
52. Miller, J. H., Fisher, D. C., Crowley, B. E., Secord, R. & Konomi, B. A. Male mastodon landscape use changed with maturation (late Pleistocene, North America). *Proc. Natl. Acad. Sci.* **119**, e2118329119 (2022).
53. Widga, C., Walker, J. D. & Stockli, L. D. Middle Holocene *Bison* diet and mobility in the eastern Great Plains (USA) based on $\delta^{13}C$, $\delta^{18}O$, and $^{87}Sr/^{86}Sr$ analyses of tooth enamel carbonate. *Quat. Res.* **73**, 449–463 (2010).
54. Prothero, D. R. *The Evolution of North American Rhinoceroses* (Cambridge University Press, 2005).
55. Tedford, R. H. et al. Mammalian biochronology of the Arikareean through Hemphillian interval (late Oligocene through early Pliocene epochs). In *Late Cretaceous and Cenozoic Mammals of North America: Biostratigraphy and Geochronology* 569 (Columbia University Press, 2004).
56. Mead, A. J. Sexual dimorphism and paleoecology in *Teleoceras*, a North American Miocene rhinoceros. *Paleobiology* **26**, 689–706 (2000).
57. Voorhies, M. R. & Stover, S. G. An articulated fossil skeleton of a pregnant rhinoceros, *Telecoeras major* Hatcher. *Proc. Neb. Acad. Sci.* **88**, 47–48 (1978).
58. Mihlbachler, M. C. Demography of late Miocene rhinoceroses (*Teleoceras proterum* and *Aphelops malacorhinus*) from Florida: linking mortality and sociality in fossil assemblages. *Paleobiology* **29**, 412–428 (2003).
59. Voorhies, M. R. A Miocene rhinoceros herd buried in volcanic ash. *Natl. Geogr. Soc. Res. Rep.* **19**, 671–688 (1985).
60. Mead, A. J. Enamel hypoplasia in Miocene rhinoceroses (*Teleoceras*) from Nebraska: evidence of severe physiological stress. *J. Vertebr. Paleontol.* **19**, 391–397 (1999).
61. Böhmer, C., Heissig, K. & Rössner, G. E. Dental eruption series and replacement pattern in Miocene *Prosantorhinus* (Rhinocerotidae) as revealed by macroscopy and x-ray: implications for ontogeny and mortality profile. *J. Mamm. Evol.* **23**, 265–279 (2015).
62. Goddard, J. Age criteria and vital statistics of a black rhinoceros population. *East Afr. Wildl. J.* **8**, 105–121 (1970).
63. Hutchins, M. & Kreger, M. D. Rhinoceros behaviour: implications for captive management and conservation. *Int. Zoo Yearb.* **40**, 150–173 (2006).
64. Laurie, A. Behavioural ecology of the greater one-horned rhinoceros (*Rhinoceros unicornis*). *J. Zool.* **196**, 307–341 (1982).
65. Dinerstein, E. Sexual dimorphism in the greater one-horned rhinoceros (*Rhinoceros unicornis*). *J. Mammal.* **72**, 450–457 (1991).
66. Shrader, A. & Owen-Smith, N. The role of companionship in the dispersal of white rhinoceroses (*Ceratotherium simum*). *Behav. Ecol. Sociobiol.* **52**, 255–261 (2002).
67. Voorhies, M. R. & Thomasson, J. R. Fossil grass anthoecia within Miocene rhinoceros skeletons: diet in an extinct species. *Science* **206**, 331–333 (1979).
68. Mihlbachler, M. C., Campbell, D., Chen, C., Ayoub, M. & Kaur, P. Microwear–mesowear congruence and mortality bias in rhinoceros mass-death assemblages. *Paleobiology* **44**, 131–154 (2018).
69. Mallet, C., Billet, G., Cornette, R. & Houssaye, A. Adaptation to graviportality in Rhinocerotoidea? An investigation through the long bone shape variation in their hindlimb. *Zool. J. Linn. Soc.* **20**, 1–37 (2022).
70. Tsutaya, T. & Yoneda, M. Reconstruction of breastfeeding and weaning practices using stable isotope and trace element analyses: A review. *Am. J. Phys. Anthropol.* **156**, 2–21 (2015).
71. Green, D. R. et al. Synchrotron imaging and Markov Chain Monte Carlo reveal tooth mineralization patterns. *PLoS One* **12**, e0186391 (2017).
72. Tafforeau, P., Bentaleb, I., Jaeger, J.-J. & Martin, C. Nature of laminations and mineralization in rhinoceros enamel using histology and X-ray synchrotron microtomography: Potential implications for palaeoenvironmental isotopic studies. *Palaeogeogr. Palaeoclimatol. Palaeoecol.* **246**, 206–227 (2007).
73. Green, D. R. et al. Quantitative reconstruction of seasonality from stable isotopes in teeth. *Geochim. Cosmochim. Acta* **235**, 483–504 (2018).
74. Yang, D. et al. Strontium isotope mapping of elephant enamel supports an integrated microsampling-modelingworkflow to reconstruct herbivore migrations. *Commun. Biol.* **8**, 274 https://doi.org/10.31219/osf.io/wzagt. (2025).
75. Reich, M. S., Flockhart, D. T. T., Norris, D. R., Hu, L. & Bataille, C. P. Continuous-surface geographic assignment of migratory animals using strontium isotopes: A case study with monarch butterflies. *Methods Ecol. Evol.* **12**, 2445–2457 (2021).
76. Baumann, E. J. & Crowley, B. E. Stable isotopes reveal ecological differences amongst now-extinct proboscideans from the Cincinnati region, USA. *Boreas* **44**, 240–254 (2015).
77. Szpak, P., Metcalfe, J. Z. & Macdonald, R. A. Best practices for calibrating and reporting stable isotope measurements in archaeology. *J. Archaeol. Sci. Rep.* **13**, 609–616 (2017).
78. R Core Team. R: A language and environment for statistical computing. R Foundation for Statistical Computing. (2022).
79. Pohlert T. PMCMRplus: Calculate Pairwise Multiple Comparisons of Mean Rank Sums Extended. (2023).
80. Widga, C., Walker, J. D. & Boehm, A. Variability in bioavailable $^{87}Sr/^{86}Sr$ in the North American midcontinent. *Open Quat.* **3**, 1–7 (2017).
81. Fox, D. L. & Fisher, D. C. Stable isotope ecology of a late Miocene population of *Gomphotherium productus* (Mammalia, Proboscidea) from port of entry pit, Oklahoma, USA. *PALAIOS* **16**, 279 (2001).
82. Lugli, F., Cipriani, A., Peretto, C., Mazzucchelli, M. & Brunelli, D. In situ high spatial resolution 87Sr/86Sr ratio determination of two middle Pleistocene (c.a. 580 ka) *Stephanorhinus hundsheimensis* teeth by LA–MC–ICP–MS. *Int. J. Mass Spectrom.* **412**, 38–48 (2017).
83. Crowley, B. E., Bruff Simpson, E. M., Hammer, S. J., Smith, J. M. & Johnson, T. M. Comparison of powdered enamel sample pretreatment methods for strontium isotope analysis. *Front. Environ. Chem.* **4**, 1114807 (2023).
84. Yang, D. et al. BITS: A Bayesian isotope turnover and sampling model for strontium isotopes in proboscideans and its potential utility in movement ecology. *Methods Ecol. Evol.* **14**, 2800–2813 (2023).
85. Britton, K., Grimes, V., Dau, J. & Richards, M. P. Reconstructing faunal migrations using intra-tooth sampling and strontium and oxygen isotope analyses: a case study of modern caribou (*Rangifer tarandus granti*). *J. Archaeol. Sci.* **36**, 1163–1172 (2009).
86. Ofstad, E. G., Herfindal, I., Solberg, E. J. & Sæther, B.-E. Home ranges, habitat and body mass: simple correlates of home range size in ungulates. *Proc. R. Soc. B Biol. Sci.* **283**, 20161234 (2016).
87. Fritsch, C. J. A., Plebani, M. & Downs, C. T. Inundation area drives hippo group aggregation and dispersal in a seasonal floodplain system. *Mamm. Biol.* **102**, 1811–1821 (2022).
88. Zachos, J. Trends, rhythms, and aberrations in global climate 65 Ma to present. *Science* **292**, 686–693 (2001).
89. Guernsey, N. C., Lohse, K. A. & Bowyer, R. T. Rates of decomposition and nutrient release of herbivore inputs are driven by habitat microsite characteristics. *Ecol. Res.* **30**, 951–961 (2015).
90. McNaughton, S. J. Grazing as an optimization process: Grass-ungulate relationships in the Serengeti. *Am. Nat.* **113**, 691–703 (1979).

91. Linklater, W. L. & Cameron, E. Z. Social dispersal but with philopatry reveals incest avoidance in a polygynous ungulate. *Anim. Behav.* **77**, 1085–1093 (2009).
92. Monard, A.-M., Duncan, P. & Boy, V. The proximate mechanisms of natal dispersal in female horses. *Behaviour* **133**, 1095–1124 (1996).
93. Stratford, K. J. et al. Female southern white rhinoceros can select mates to avoid inbreeding. *J. Hered.* **112**, 385–390 (2021).
94. Wilson, S. G., Hockings, G., Deretic, J.-A.M. & Kark, S. More than just mud: the importance of wallows to Javan rhino ecology and behaviour. *Pachyderm* **61**, 49–62 (2020).

Acknowledgements

We thank the staff of the Division of Vertebrate Paleontology at the University of Nebraska State Museum for their assistance with this project. We also thank T. Johnson at the University of Illinois Urbana-Champaign for conducting Sr isotope and concentration analyses, and J. Curtis at the University of Florida for C and O isotope analyses. Thank you to R. M. Joeckel, J. Miller, E. Simpson, A. Hensley, X. Zheng, and C. Widga for providing conceptual, methodological, analytical, and statistical advice, and two anonymous reviewers who helped strengthen this manuscript. Lastly, this project was funded by a Geological Society of America Charles A. & June R. P. Graduate Student Research Grant, a Western Interior Paleontological Society Karl Hirsch Memorial Grant, a University of Cincinnati Chapter of Sigma Xi Grant-in-aid of Research, endowment funding from the University of Cincinnati Geosciences Department (all to CTW), and the University of Nebraska State Museum Meek Fund (to RS).

Author contributions

All authors contributed to the conceptualization and design of this project. CTW and RS acquired funding. CTW performed the formal analyses, curated data, and wrote the original draft. BEC and RS provided lab space, resources, and supervision, and contributed editorial advice.

Declarations

Competing interests

The authors declare no competing interests.

Additional information

Supplementary Information The online version contains supplementary material available at https://doi.org/10.1038/s41598-025-94263-z.

Correspondence and requests for materials should be addressed to C.T.W.